

**NASA TECHNICAL
MEMORANDUM**

NASA TM X- 73,197

NASA TM X- 73,197

EFFECTS OF SPOILERS AND GEAR ON B-747

WAKE VORTEX VELOCITIES

**A. B. Luebs, J. G. Bradfute, and
D. L. Ciffone**

**Ames Research Center
Moffett Field, Calif. 94035**

**(NASA-TM-X-73197) EFFECTS OF SPOILERS AND
GEAR ON B-747 WAKE VORTEX VELOCITIES (NASA)
25 p HC A02/MF A01 CSCL 01A**

N77-18052

**G3/02 Unclass
17197**

August 1976

**MAR 1977
RECEIVED
NASA STI FACILITY
INPUT BRANCH**

1. Report No. NASA TM X-73,197		2. Government Accession No.		3. Recipient's Catalog No.	
4. Title and Subtitle EFFECTS OF SPOILERS AND GEAR ON B-747 WAKE VORTEX VELOCITIES				5. Report Date	
				6. Performing Organization Code	
7. Author(s) A. B. Luebs,* J. G. Bradfute, [†] and D. L. Ciffone				8. Performing Organization Report No. A-6881	
9. Performing Organization Name and Address Ames Research Center Moffett Field, California 94035				10. Work Unit No. 514-52-01	
				11. Contract or Grant No.	
12. Sponsoring Agency Name and Address National Aeronautics and Space Administration Washington, D. C. 20546				13. Type of Report and Period Covered Technical Memorandum	
				14. Sponsoring Agency Code	
15. Supplementary Notes *Graduate Student, Stanford University, Stanford, Calif. [†] Student, Harvey Mudd College, Claremont, Calif.					
16. Abstract In support of the NASA wake vortex alleviation program, vortex velocities were measured in the wakes of four configurations of a 0.61-m (2-ft) span model of a B-747 aircraft. The wakes were generated by towing the model underwater in a ship model basin. Tangential (vertical) and axial (streamwise) velocity profiles were obtained with a scanning laser velocimeter as the wakes aged to 35 span lengths behind the model. A 45° deflection of two outboard flight spoilers with the model in the landing configuration resulted in a 36 percent reduction in wake maximum tangential velocity, altered velocity profiles, and erratic vortex trajectories. Deployment of the landing gear with the inboard flaps in the landing position and outboard flaps retracted had little effect on the flap vortices to 35 spans, but caused the wing tip vortices to have: (1) more diffuse velocity profiles; (2) a 27 percent reduction in maximum tangential velocity; and (3) a more rapid merger with the flap vortices.					
17. Key Words (Suggested by Author(s)) Multiple vortex wakes Wake vortex velocities Laser velocimeter measurements				18. Distribution Statement Unlimited STAR Category - 02	
19. Security Classif. (of this report) Unclassified		20. Security Classif. (of this page) Unclassified		21. No. of Pages 25	
				22. Price* \$3.25	

SYMBOLS

b	wing span, 0.61 m
C_L	lift coefficient
f	LV signal frequency
f_s	LV Bragg Cell shifted frequency
LDG	landing configuration, trailing-edge flaps deflected 46° , leading-edge flaps deployed
LDG (S)	same as LDG but with spoilers deflected upward 45°
LDG/O	same as LDG but with outboard trailing-edge flaps retracted
LDG/O (GR)	same as LDG/O but with landing gear retracted
LV	laser velocimeter
U_∞	towing speed, m/sec
V_x	vortex axial (streamwise) velocity component
V_z	vortex tangential (vertical) velocity component
X	streamwise position, positive downstream of wingtip trailing edge
Y	spanwise position, positive outboard from fuselage centerline in direction of right semispan
Z	vertical position, positive upward from wingtip trailing edge
α	model angle of attack
Δ	unit change
θ	intersection angle of the crossed laser beams
μ	index of refraction

EFFECTS OF SPOILERS AND GEAR ON B-747 WAKE VORTEX VELOCITIES

A. B. Luebs,* J. G. Bradfute,[†] and D. L. Ciffone

Ames Research Center

SUMMARY

In support of the NASA wake vortex alleviation program, vortex velocities were measured in the wakes of four configurations of a 0.61-m (2-ft) span model of a B-747 aircraft. The wakes were generated by towing the model underwater in a ship model basin. Tangential (vertical) and axial (streamwise) velocity profiles were obtained with a scanning laser velocimeter as the wakes aged to 35 span lengths behind the model. A 45° deflection of two outboard flight spoilers with the model in the landing configuration resulted in a 36 percent reduction in wake maximum tangential velocity, altered velocity profiles, and erratic vortex trajectories. Deployment of the landing gear with the inboard flaps in the landing position and outboard flaps retracted had little effect on the flap vortices to 35 spans, but caused the wing tip vortices to have: (1) more diffuse velocity profiles; (2) a 27 percent reduction in maximum tangential velocity; and (3) a more rapid merger with the flap vortices.

INTRODUCTION

This experimental study is part of a concerted effort to reduce the hazard potential of lift-generated wake vortices trailing heavy aircraft. Recent research (ref. 1) has established that turbulence produced by flight spoilers and favorable span load gradients induced by selective flap settings are effective in alleviating concentrated wake vorticity. Both of these concepts have been shown (ref. 1) to be applicable to the B-747 airplane. However, it is not completely understood how landing gear deployment can adversely affect wake alleviation obtained by span load modification (ref. 1) or what flow mechanisms are responsible for the alleviation achieved with properly placed spoilers (ref. 2).

To help clarify these uncertainties, this paper presents quantitative measurements obtained in the wake downstream of a B-747 aircraft model configured with spoilers and flaps to alleviate concentrated wake vorticity. The experiment was performed in the University of California's ship model basin at Richmond, California. Time-dependent tangential (vertical) and

*Graduate Student, Stanford University, Stanford, Calif.

[†]Student, Harvey Mudd College, Claremont, Calif.

axial (streamwise) velocity distributions in the wakes of a 0.61-m (2-ft) span model were measured with a scanning laser velocimeter. Data were obtained to distances of 35 span lengths behind the model. The model was fitted with removable triple-slotted flaps, flight spoilers, and landing gear. The mean chord test Reynolds number was 82,000.

EXPERIMENTAL APPARATUS AND PROCEDURE

Facility and Model Description

The University of California's ship model basin, located in Richmond, California, is 61 m long, 2.44 m wide, and 1.7 m deep. The model was strut-mounted to an electrically driven carriage and towed through the water past a viewing station (fig. 1). At this station, large glass windows in the side of the tank allow the model wake to be observed as it ages and descends. All data were obtained at a towing speed of 1 m/sec.

Four configurations of a 0.01 scale model of a B-747 aircraft were tested (fig. 2): (1) landing, LDG, with inboard and outboard flaps deflected 46° and leading-edge flaps extended; (2) LDG (S), same as LDG but with two outboard flight spoilers deflected upward at 45° ; (3) LDG/O, same as LDG but with outboard flaps retracted; and (4) LDG/O (CR), same as LDG/O but with landing gear retracted. The spoilers were located forward of the outboard half of the outboard flap from 0.59 to 0.69 of the semispan (fig. 2). To allow observation of the wake vortices that it generates in the water, the model is equipped with dye-ejection orifices (ref. 3).

Experimental Procedure

It has been concluded that the scaling laws for modeling fluid phenomena, pertinent to the study of wake vortices, are essentially the same for tests in water as in air (refs. 4-7), and that the forces acting on hydrofoils operated at depths greater than two chord lengths are essentially unaffected by the free surface and are equal to those obtained on a wing operating in an infinite medium (ref. 8). The model centerline in these tests was located approximately five chord lengths (0.75 of a span) below the free surface. Although the test Reynolds number (82,000 based on chord) was considerably less than full scale, general agreement in wake appearance (ref. 1) and vortex trajectories (ref. 9) was evident where comparisons could be made with flight data. Wake data obtained in this test should, therefore, be indicative of flight results. This seeming lack of Reynolds number sensitivity does not come as a complete surprise since previous wake vortex velocity measurements obtained in this facility (ref. 5) on a variety of wing configurations correlated well (ref. 10) with both wind-tunnel and flight measurements.

Dye was emitted from the model to allow visual tracking of the wake vortices as they moved through the water. In addition, the viewing section

of the tank was seeded with polystyrene copolymer latex spheres to provide sufficient scattering particles to ensure laser velocimeter signals with adequate strength and resolution. The combination of a small particle size (2 to 15 μ diameter) and a specific gravity of 1.06 for these spheres ensures flow-tracing fidelity. The laser velocimeter began scanning the flow field prior to the model's arrival at the viewing station, and the timing for a run was initiated as the streamlined strut passed the outgoing laser beams. During each run, the elevation of the laser velocimeter was kept constant and the aging vortices allowed to descend through the LV's optical axis. After each run, the carriage was returned to the starting end of the tank, and the laser was used to monitor water motion to ensure a calm tank prior to the next run (eddy velocities ≤ 0.004 m/sec). At a towing speed of 1 m/sec, the laser scanning rate was such that the rate of change of the age of the wake with lateral position of the focal point of the laser beams was $\Delta(X/b)/\Delta(Y/b/2) = 2$. Hence, during the scan of the vortex cores, the wake aged approximately one-third of a span (~ 0.2 sec).

Data Acquisition and Presentation

The trailing vortex flow was spatially scanned using the single component laser velocimeter shown installed at the viewing station of the tank, in figure 1, and schematically in figure 3. A prism splits the green (5145 Å) output beam of the argon-ion laser into two parallel beams, one of which is then frequency-shifted 40 MHz by a Bragg Cell to achieve directional sensitivity in the signal. The two beams then pass through a scanning lens, which is mounted on a motorized slide, and are subsequently crossed at a focal point in the water by the collector lens. The beam splitter prism and Bragg Cell can be rotated as a unit to measure vertical or streamwise flow velocities. Light scattered from particles at the focal point is collected through the same optical system and focused onto a photomultiplier tube. The frequency detected by the photomultiplier is linearly related to flow-field velocity by

$$V = \frac{(5145 \text{ Å})(f - f_s)}{2\mu \sin \theta/2}$$

where f_s is the Bragg Cell shift frequency, 40 MHz. This equation represents the vortex axial velocity V_x or tangential velocity, V_z (depending on the orientation of the LV) when a core centerline penetration of the vortex is achieved. The crossing angle θ of the two laser beams and the distance of their focal point from the tank wall are dependent on the scanning lens position. The index of refraction of water was used in the above equation ($\mu = 1.33$).

A spectrum analyzer and signal sampler were used to process the photomultiplier output signal. The signal sampler provided an analog output proportional to frequency. This voltage, together with the voltage across potentiometers mounted on the scanning lens mechanism and the lift supporting the laser, was digitized and recorded on tape. During the interval between test runs, while water motions were settling, the data stored on tape from

the just-completed test run were reduced and plotted. This onsite data review capability greatly assists in providing representative data in a minimum amount of test runs, and allows for further investigation of unexpected results.

Flow field velocities are presented as fractions of towing speed U_{∞} . Streamwise position X (positive downstream), spanwise position Y (positive outboard along the right semispan), and vertical position Z (positive upward) are nondimensionalized by wingspan b . The origin of these coordinates is the projected location of the wingtip trailing edge onto the fuselage centerline.

DISCUSSION OF RESULTS

The wakes of four configurations of the B-747 model were investigated. Velocity profiles through the wake vortices were measured and compared at three vertical positions below the model. These positions were $Z/b = -0.16$ (nearfield), -0.44 (midfield), and -0.69 (farfield). Of primary interest was the effect of spoilers on the LDG configuration and the effect of landing gear on the LDG/O configuration. The results are presented as: (a) tangential and axial velocity profiles for the dominant vortices (figs. 5-8); maximum vortex velocity downstream dependence (figs. 9 and 10); and (c) vortex trajectories (figs. 11 and 12).

Vortex Velocity Profiles

In the landing configuration, the B-747 sheds five vortices from each side of the wing. Four of these vortices are due to the span-loading gradients caused by the flaps and the fifth is due to the span-load gradient at the wing tip. The dominant vortex is shed from the outboard edge of the outboard flap. The wing tip vortex merges with this vortex, and the result is a persistent vortex. It has been established (ref. 1) that a 45° deflection of the two outboard flight spoilers (fig. 2) results in a 15 to 50 percent reduction of the rolling moment on an encountering aircraft, depending on the wing span ratio of generator to follower (refs. 1,2). However, the mechanism of interaction between spoiler and vortex is not completely understood.

The measured effect of spoilers on the tangential velocity profile of the dominant vortex in the wake of the LDG configuration is shown in figure 5. The models' two outboard flight spoilers were deflected upward 45° . Lift coefficient with and without spoilers was kept at a nominal value of 1.3 by adjusting model angle of attack. In the nearfield (at $Z/b = -0.16$), the spoilers increase the vortex sink rate by an average of 48 percent and reduce the maximum tangential velocity by 28 percent.¹ Hence, with spoilers, the

¹ Maximum tangential velocity is defined as the average value of inboard and outboard peak tangential velocity from a given velocity profile. Vortex sink rate is estimated from the position of the vortex center with respect to zero velocity.

flap vortex arrives at this nearfield vertical station two span lengths sooner and has a lower tangential velocity. Negative vertical velocity components resulting from the downward motion of the vortex cause the velocity profile to be biased downward toward negative values of tangential velocity. The data of figure 5 have not been corrected for this motion. Although the saddle shape of the velocity profile at the 0.7 semispan position for the LDG (S) configuration appears at a spanwise location just behind the outboard edge of the spoilers, it is believed that this region of low velocity is the result of the like-sign wingtip vortex merging with the flap vortex. The same depression is not seen in the LDG configuration velocity profile because, by 7.2 span lengths, the merging process has been completed (ref. 3), and only the single flap vortex is distinguishable.

In the midfield (at $Z/b = -0.44$) the average vortex sink rate of each configuration increased slightly, while their maximum tangential velocity did not change. Figure 5 shows the major effect of the spoilers at this station to be a more diffuse flap vortex with a broadened core. However, some of this broadening may be due to vortex curvature in the plane orthogonal to the one containing the laser beams. At this location below the model, the LDG (S) flap vortex is moving laterally in an erratic path toward the observation windows (vortex trajectories are discussed later). The flap and wingtip merger has been completed at this station and the saddle shape in the velocity profile of the LDG (S) configuration is no longer evident. Further downstream at $X/b = 27.2, 28.3$ and $Z/b = -0.69$, the maximum tangential velocities remain unchanged, the average vortex sink rate of the LDG (S) configuration has slowed and become comparable to that of the LDG configuration, and the velocity profile of the LDG (S) configuration shows a reconcentration of vorticity (reduced core size). While the relatively small core diameter indicated by the LDG (S) velocity profile is surprising and suggestive of an off-center core penetration, the magnitudes of tangential velocity agree with the rest of figure 5 and the apparent reconcentration of vorticity are in agreement with flow visualization studies (ref. 6).

In the LDG/O (GR) configuration, the outboard flap is retracted and three vortices are shed from each side of the wing — one from each side of the inboard flap and the wingtip. First, the vortex from the inboard side of the flap merges with the one from the flaps' outboard side (ref. 11), and then the wingtip vortex moves inboard and merges with this resulting flap vortex, causing a very diffuse residual vortex. Compared to the landing configuration, reductions of 50 percent in rolling moment on an encountering aircraft (depending on the wing span ratio of generator to follower) have been measured for this LDG/O (GR) configuration (ref. 1). However, it is not completely understood why the vortex reconcentrates when the landing gear is deployed.

The measured effect of landing gear is shown in a comparison of the LDG/O (GR) vortex velocity profiles of figures 6 to 8. Tangential velocity profiles from the outboard vortex of the flap and from the wingtip are compared in figures 6 and 7, respectively, while figure 8 compares flap axial velocity profiles. Lift coefficient was 1.16 for all of this data. Although reference 11 suggests a difference in the merging characteristics of the flap

vortices due to the presence of the landing gear. Figure 6 indicates that within the scatter of the data, the landing gear does not appear to affect either the magnitude or profile of the flap vortex tangential velocity to 29 span lengths behind the model. This vortex is quite concentrated and has high tangential velocities in the nearfield. The upwash seen in the velocity profile in the vicinity of the wingtip for the LDG/O configuration at $Z/b = -0.44$ and -0.69 is probably associated with residual velocities from the wingtip vortex after merger with the flap. This merger is completed by about 21 spans. The presence of the landing gear does affect the wingtip vortex velocity profile in this configuration. This is shown in figure 7. At 7 to 8 spans behind the model, the wingtip vortex is located above and inboard of the flap vortex (ref. 3) and is moving rapidly downward. This rapid downward movement $V_z/U_\infty \approx -0.075$ is the reason that the measured velocity profiles at $Z/b = -0.154$ are almost entirely negative. For the LDG/O (GR) configuration, the wingtip vortex is very concentrated and well-defined. The presence of the landing gear makes the vortex more diffuse and reduces its maximum tangential velocity by 27 percent. The upwash evident in the velocity profile over the outer half of the semispan is due to circulation from the flap vortex, which is outboard and below the tip vortex. At 12 span lengths behind the model, the wingtip vortex has moved downward to a position almost directly inboard of the flap vortex. The increased fluctuations in the velocity profiles over the outboard section of the semispan are due to the closer proximity of the flap vortex. Due to the gear, the LDG/O tip vortex is still more diffuse and has lower tangential velocities than the LDG/O (GR) configuration. At this station, the LDG/O tip vortex is also farther outboard, which is consistent with flow visualization results (ref. 3). These flow visualization studies also indicate that the wingtip vortex merges with the flap vortex at ~18 span lengths when the gear is deployed and is delayed to ~21 spans when the gear is retracted. Figure 7 suggests this at a vertical position of 0.69 span below the model where a wingtip vortex tangential velocity profile was measured for the LDG/O (GR) configuration at 21.4 spans, but none was measurable for the gear-retracted configuration. At this station, the LDG/O (GR) wingtip vortex is below and outboard of the flap vortex, the location where merger generally occurs (ref. 3).

Axial velocity profiles of the flap vortex for the LDG/O and LDG/O (GR) configurations are shown in figure 8. Since this laser velocimeter can measure only one velocity component at a time, these profiles were taken separately from the data of figure 6. It is seen that at $Z/b = -0.16$, the flap outboard edge vortex has a clearly defined axial velocity defect. An axial velocity defect being defined as $(1 - V_x/U_\infty) > 1.0$ and representing a streamwise flow in the core of the vortex in an upstream direction towards the model. Figure 8 shows that by the time this vortex has descended to 0.44 span below the model, fluctuations appear in the axial velocity profile for the LDG/O (GR) configuration. These fluctuations are a consequence of the wingtip vortex-flap vortex merger. For the LDG/O (GR) configuration, the merger is in its final stages and a double peak is seen in the velocity profile. Axial velocities for the LDG/O configuration were measured at earlier times at this vertical station, and the merging process was not as far along. The maximums in velocity at 0.55 and 0.8 semispan is due to the flap and wingtip vortices, respectively. Axial flow enhancement seen at

several positions along the semispan for the LDG/O configuration might be due in part to a measured axial component resulting from a downward curvature of the vortex. At $Z/b = -0.69$, there is still evidence of vortex merger in the LDG/O configuration; both velocity profiles have become quite diffuse. In summary, the effect of landing gear on the axial velocity profile of the flap outer-edge vortex appears to be a reduction in velocity defect and a more diffuse core. The reduced velocity defect is surprising, since it was anticipated that the gear drag would result in an increased axial velocity defect. Perhaps the momentum defect associated with the gear does not become transported into the vortex core until further downstream.

Vortex Maximum Velocities

Comparisons of the downstream dependence of vortex maximum tangential velocity normalized by lift coefficient, for the configurations tested, is presented in figure 9. The velocities of the outboard flap outer-edge vortex for both the LDG and the LDG (S) configurations display the now familiar plateau (ref. 5). Although, for these configurations, there is little decay in the normalized maximum velocities once wake rollup and merging have been completed ($-X/b > 6$), the spoilers reduce this velocity by 35 percent. In contrast, there is little, if any, effect of the landing gear on the maximum velocity of the inboard flap outer-edge vortex, and no plateau region is evident for this vortex. The absence of the plateau is due to the longer time required for the wingtip-flap vortex merger. The flow visualization indicates that this merger is not completed until ~ 18 to 20 span lengths downstream, and the velocity profiles (fig. 6) suggest that it may go on longer than that. At 30 span lengths downstream, the wake maximum tangential velocity of the LDG/O and LDG (S) configurations is comparable. However, there is evidence (refs. 1,7) that further downstream the LDG/O flap vortex experiences a reconcentration of vorticity. Also shown in figure 9 is the LDG/O laser velocimeter wind tunnel result of reference 12. The agreement with the present measurements is surprisingly good (within 17 percent) considering the difficulty of making these nearfield measurements.

A limited number of streamwise velocities were measured for the LDG, LDG/O and LDG/O (GR) configurations. The variation of flap vortex maximum axial velocity defect with downstream distance for these configurations is shown in figure 10. The vortex core streamwise velocity towards the model for the LDG configuration remains constant at about 12 percent of the towing speed from 5 to 25 spans behind the model. For the LDG/O and LDG/O (GR) configurations, the vortex axial velocity defect is 50 percent higher in the nearfield, prior to merger of the flap and wingtip vortex.

Vortex Trajectories

Although the primary purpose of this experiment did not include obtaining vortex trajectory information, vortex-position time-histories can be helpful in explaining the measured velocity profiles. Vortex trajectories can be only roughly deduced from velocity measurements at just three

elevations below the model. For this reason, the trajectory information presented in figures 11 and 12 has been supplemented with the flow visualization data of reference 6. These figures relate prominent vortex spanwise and vertical location. Figure 11 shows what effect two outboard flight spoilers have on the trajectory of the vortex shed from the outboard edge of the outboard flap in the landing configuration. The laser and flow visualization data show the same general trend - with spoilers, the vortex initially moves further inboard of, then further outboard of, and eventually approaches the path of, the vortex without spoilers. The trajectory with spoilers is much more erratic and, for the first 25 spans behind the model, it descends much more rapidly (ref. 6). Figure 11 shows that at about 0.4 span below the model, the movement of this vortex in the vertical plane is almost entirely lateral in the outboard direction. Figure 12 shows the trajectories of the outboard edge flap vortex and wing tip vortex for the LDG/O and LDG/O (GR) configurations. Selected X/b's are noted on the figure to allow relative position comparisons. The effect of the landing gear on the flap vortex trajectory was negligible to 30 spans. At 12 span lengths downstream of the model, with gear deployed, the wing tip vortex begins to move outboard sooner. This is suggested by the laser data presented in the figure and is quite evident in the flow visualization data of references 6 and 7. No laser data for the wing tip vortex with gear extended is shown beyond 12 span lengths due to its accelerated outboard movement resulting in a merger with the flap vortex before the next vertical test position was reached (fig. 7). For reasons of clarity, only gear-retracted flow visualization data are presented in the figure. The agreement between the laser and flow visualization data is good.

SUMMARY AND CONCLUSIONS

The wakes of four configurations of a B-747, 0.01 scale (0.61-m span) model transport aircraft were investigated. The wake velocities were measured at three different vertical positions below the model and compared in an attempt to determine the effects of flight spoilers and landing gear. The following is a summary of the results of this experimental investigation:

- (1) At a lift coefficient of 1.3, the following changes were noted in the wake of the landing configuration when the two outboard flight spoilers were deployed at 45° deflection: (a) the maximum tangential velocity of the wake's persisting vortex (shed from the outboard edge of the outboard flap) was reduced by 36 percent from the 5 to 28 span lengths behind the model where velocities were recorded; (b) at 12 spans, the flap vortex was quite diffuse, but by 28 span lengths its vorticity appeared to be reconcentrating; (c) the vortex trajectory was more erratic, sinking almost twice as fast and moving further inboard at 5 span lengths, and then swinging further outboard at 12 span lengths. However, it eventually settled down and approached the trajectory of the unspoiled configuration by 28 span lengths. These limited results suggest that the major influence of spoilers on the wake results from their generation of turbulence.

- (2) At a lift coefficient of 1.2, the following changes were noted in the wake of the landing configuration with outboard flaps retracted, as a result of landing gear deployment: (a) the wing tip vortex was more diffuse as it orbited about the outboard edge flap vortex, its maximum tangential velocity was reduced by 27 percent, and it merged sooner with the flap vortex; (b) contrary to what was expected, the flap vortex had less of an axial velocity defect although its core was more diffuse. The weakening of the wing tip vortex appears to be associated with its passage through that portion of the wake that is transporting landing gear turbulence. This weakening results in the wing tip vortex merging sooner with the like sign flap vortex. At 29 span lengths behind the model, there was still no evidence of the residual, merged, flap vortex reconcentrating its vorticity. Hence, it is still not evident how the landing gear adversely affects the flap vortex.

REFERENCES

1. NASA Symposium on Wake Vortex Minimization. NASA SP-409, 1976.
2. Corsiglia, V. R.; and Rossow, V. J.: Wind-Tunnel Investigation of the Effect of Porous Spoilers on the Wake of a Subsonic Transport Model. NASA TM X-73,091, 1976.
3. Ciffone, D. L.: Vortex Interactions in Multiple Vortex Wakes Behind Aircraft. J. Aircraft, April 1977.
4. Kirkman, K. L.; Brown, C. E.; and Goodman, A.: Evaluation of Effectiveness of Various Devices for Attenuation of Trailing Vortices Based on Model Test in a Large Towing Basin. NASA CR-2202, 1973.
5. Ciffone, D. L.; and Orloff, K. L.: Far-Field Wake-Vortex Characteristics of Wings. J. Aircraft, vol. 12, no. 5, May 1975, pp. 464-470.
6. Ciffone, D. L.: Alleviation and Ground Plane Effects on DC-10-30 and B-747 Wakes. Paper to be presented at Conference on Aircraft Wake Vortices, March 1977, U. S. Department of Transportation.
7. Ciffone, D. L.; and Lonzo, C.: Flow Visualization of Vortex Interactions in Multiple Vortex Wakes Behind Aircraft. NASA TM X-62,459, 1975.
8. Wadlin, K. L.; Ramsen, J. A.; and McGehee, J. R.: Tank Tests at Sub-cavitation Speeds of an Aspect Ratio 10 Hydrofoil with a Single Strut. NACA RM L9K14a, 1950.
9. Brashears, M.; Zalay, A. D.; and Hallock, J.: Laser Doppler Flight Test Measurements of B-747 Wake Vortex Characteristics. Lockheed-Huntsville Research and Engineering Center. Paper to be presented at Conference on Aircraft Wake Vortices, March 1977, U. S. Department of Transportation.
10. Iversen, J. D.: Correlation of Turbulent Trailing Vortex Decay Data. J. Aircraft, vol. 13, no. 5, 1976, pp. 338-342.
11. Corsiglia, V. R.; Rossow, V. J.; and Ciffone, D. L.: Experimental Study of the Effect of Span Loading on Aircraft Wakes. J. Aircraft, vol. 13, no. 12, December 1976, pp. 968-973.
12. Corsiglia, V. R.; and Orloff, K. L.: Scanning Laser Velocimeter Surveys and Analysis of Multiple Vortex Wakes of an Aircraft. NASA TM X-73,169, 1976.

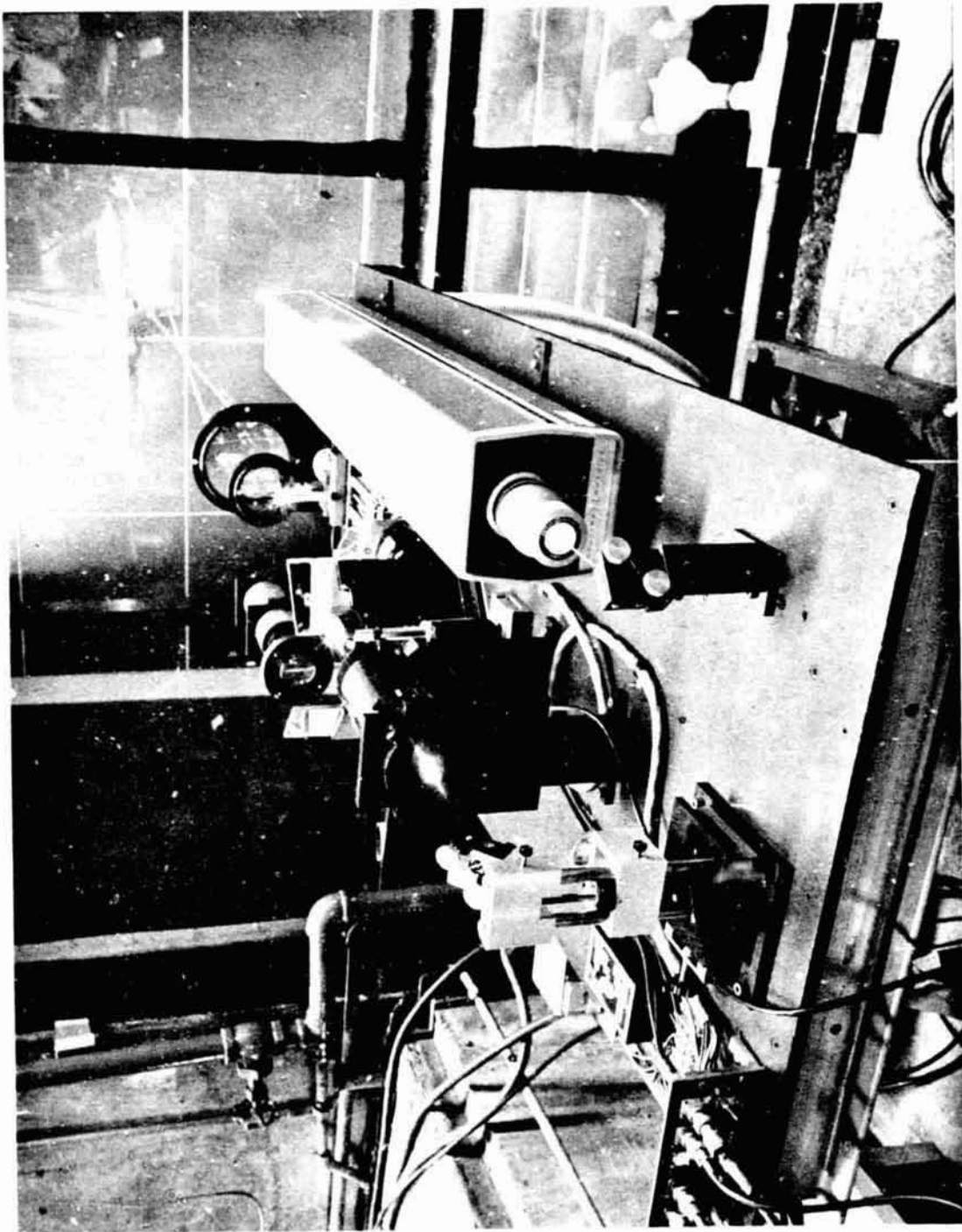
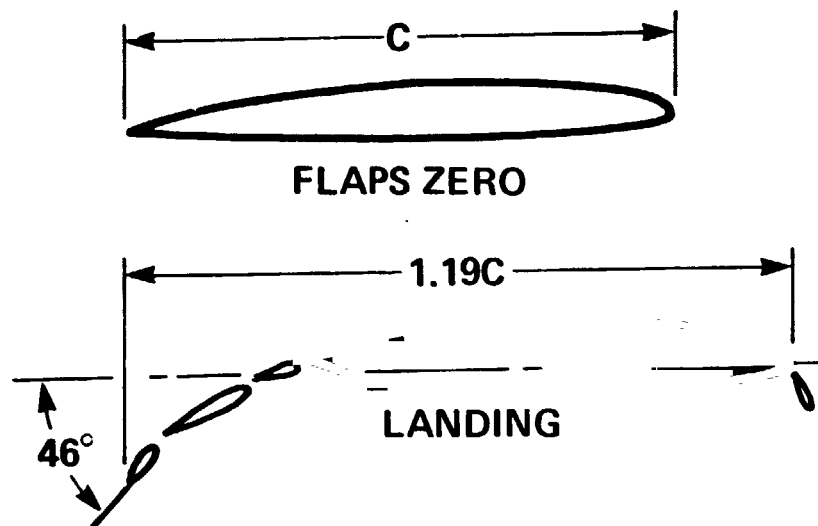
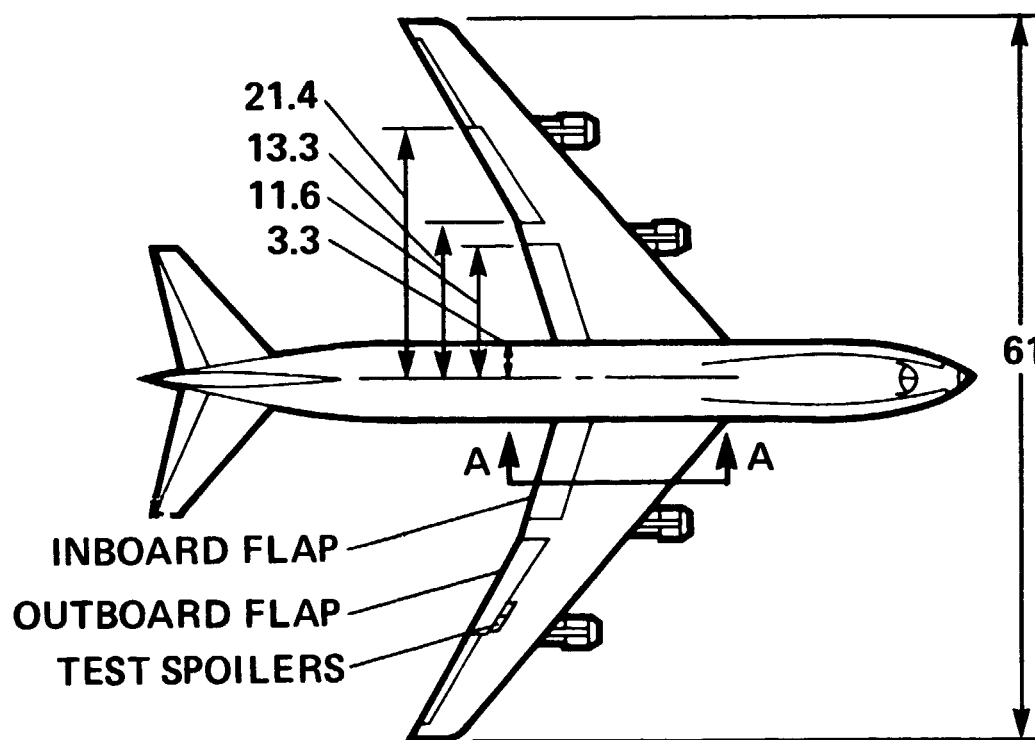


Figure 1.- Test installation photograph.



SECTION A-A DETAILS



ALL DIMENSIONS, cm

Figure 2.- 0.01 scale model of Boeing 747 airplane.

- | | |
|-------------------------------|--------------------------|
| 1. ARGON LASER (6 watt) | 7. SCANNING LENS |
| 2. MIRROR | 8. COLLECTOR LENS |
| 3. BEAM RAISER | 9. MIRROR |
| 4. BEAM SPLITTER & BRAGG CELL | 10. LENS |
| 5. MIRROR WITH 4 HOLES | 11. PHOTOMULTIPLIER TUBE |
| 6. SCANNING MECHANISM | |

— TRANSMITTED LIGHT (5145 Å, GREEN)
 --- RECEIVED LIGHT

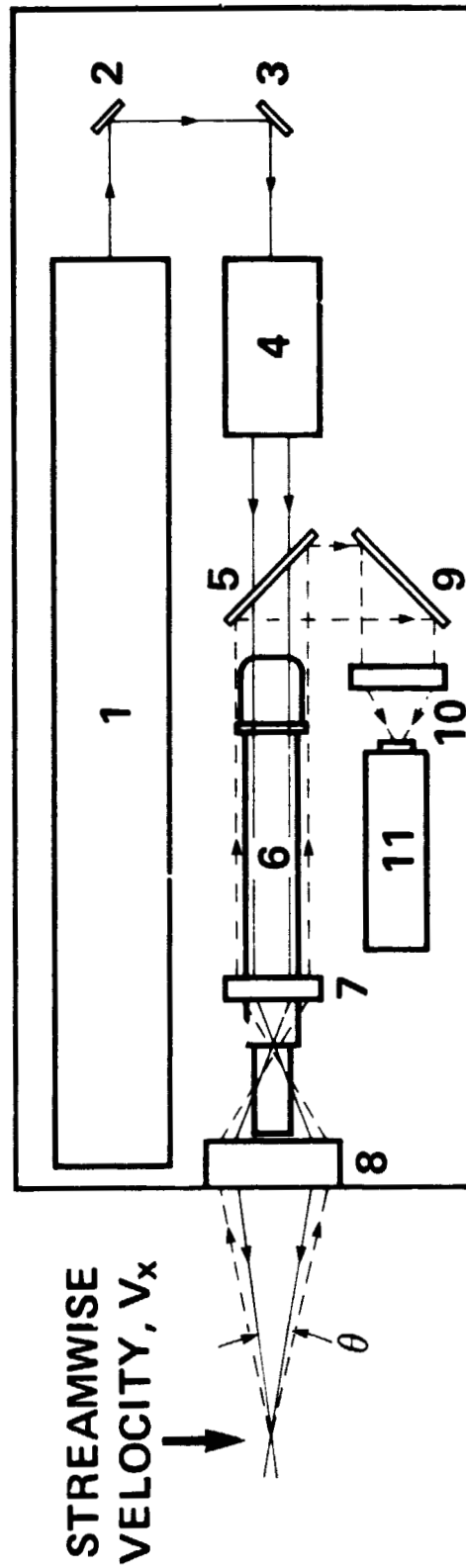


Figure 3.- Data acquisition and reduction system schematic.

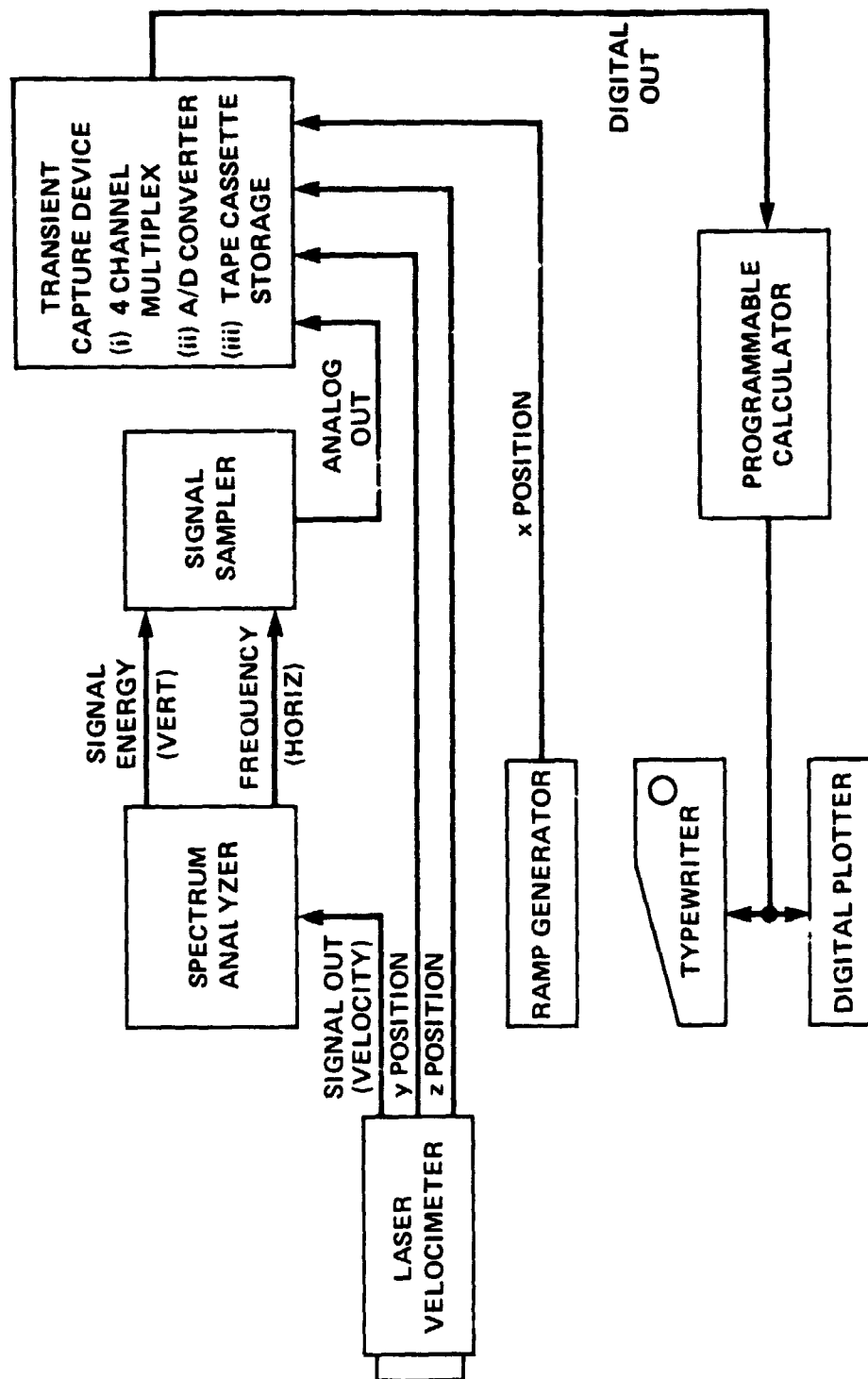


Figure 4.- Laser velocimeter schematic. Parallel light beams oriented to measure streamwise velocity.

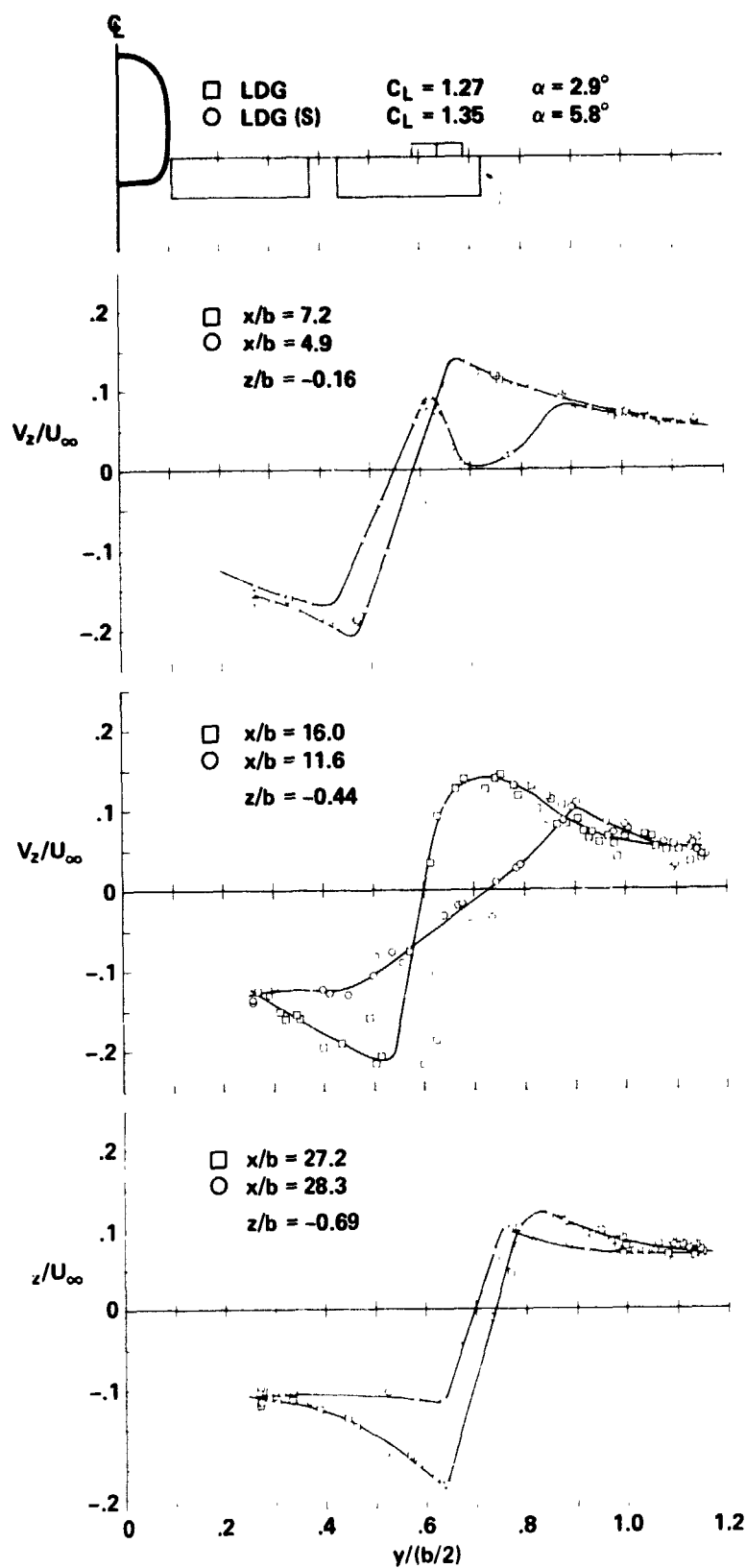


Figure 5.- Effect of flight spoilers on flap vortex tangential velocity profile. Landing configuration.

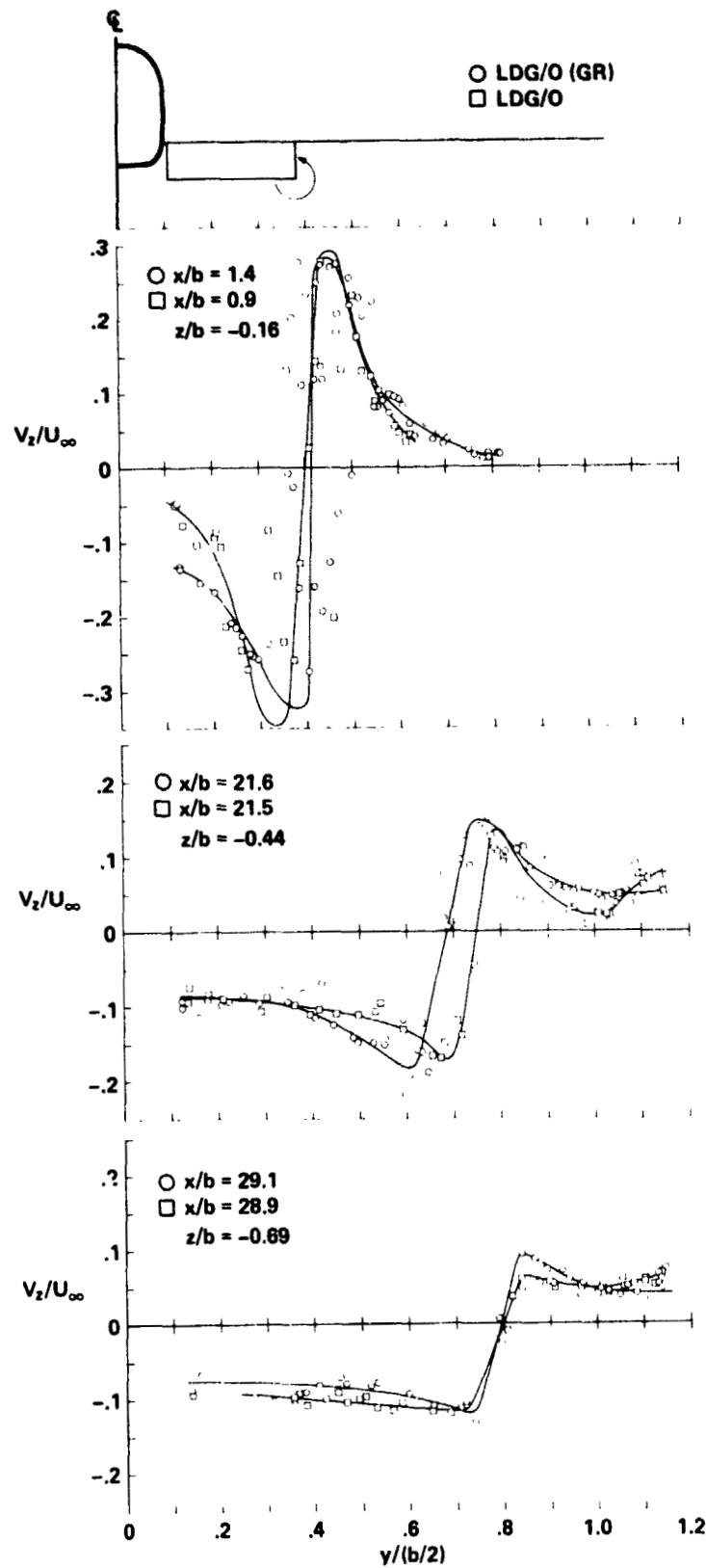


Figure 6.- Effect of landing gear on flap vortex tangential velocity profile.
LDG/O configuration, $C_L = 1.16$, $\alpha = 5.8^\circ$.

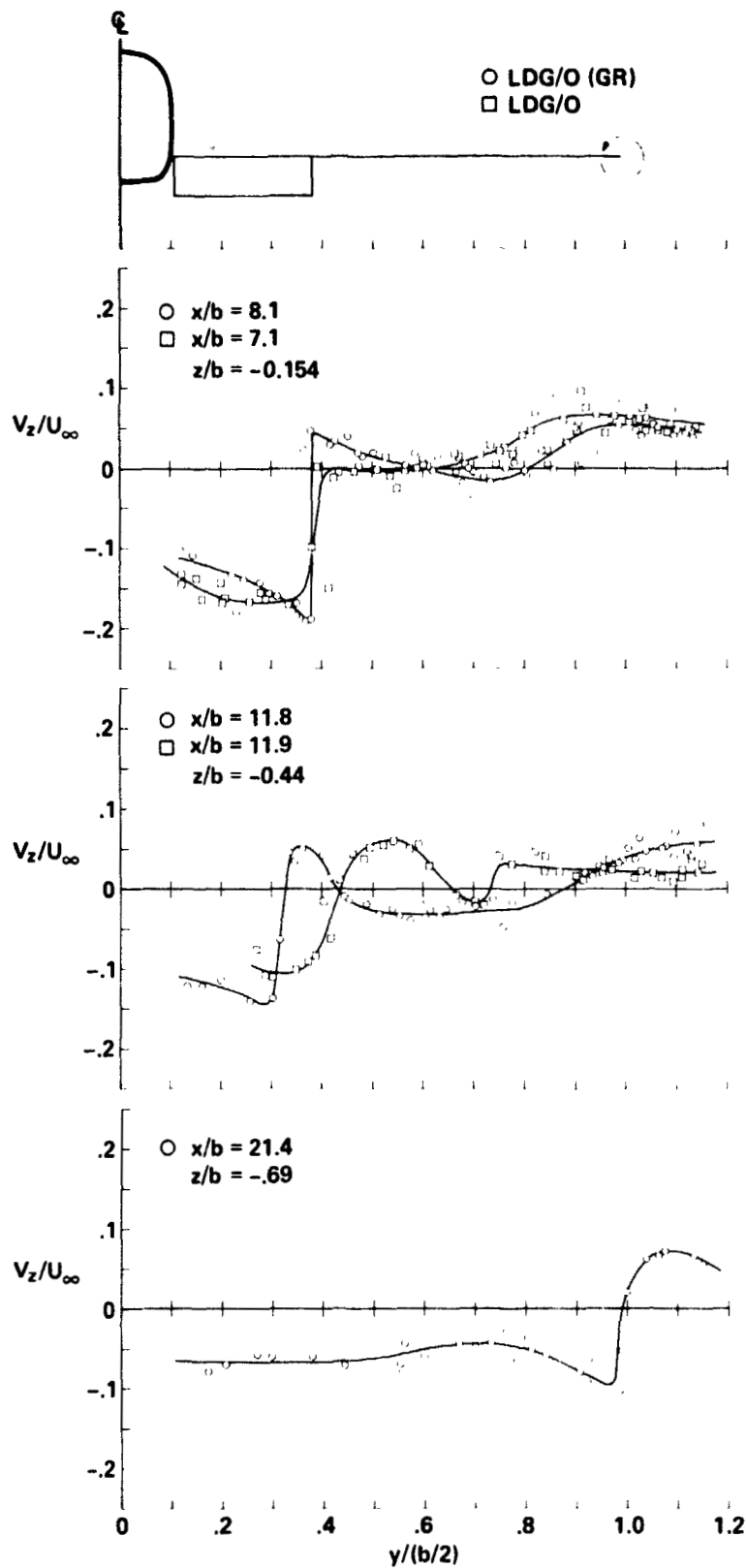


Figure 7.- Effect of landing gear on wing tip vortex tangential velocity profile. LDG/O configuration, $C_L = 1.16$, $\alpha = 5.8^\circ$.

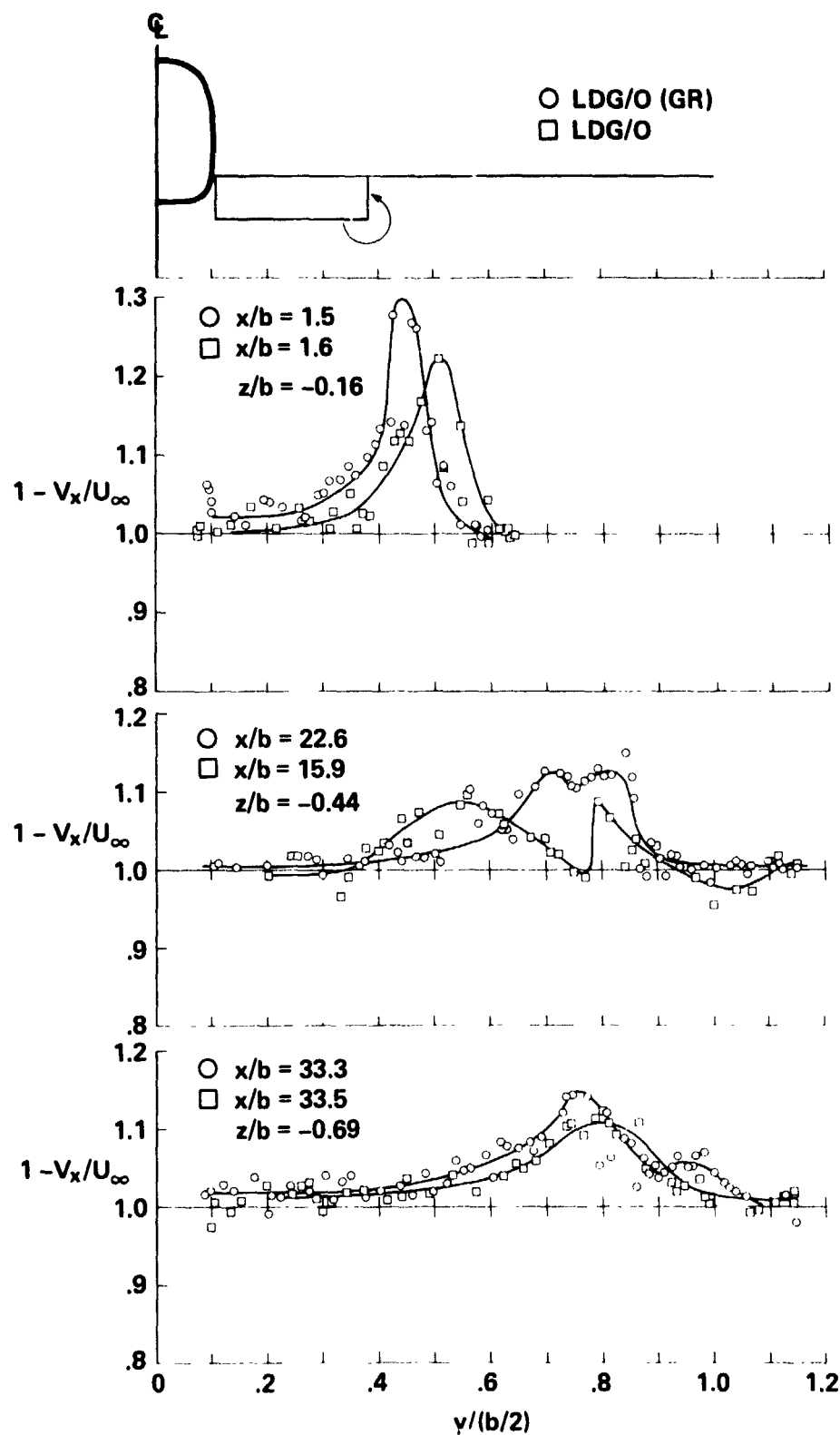


Figure 8.- Effect of landing gear on flap vortex axial velocity profile.
LDG/O configuration, $C_L = 1.16$, $\alpha = 5.8^\circ$.

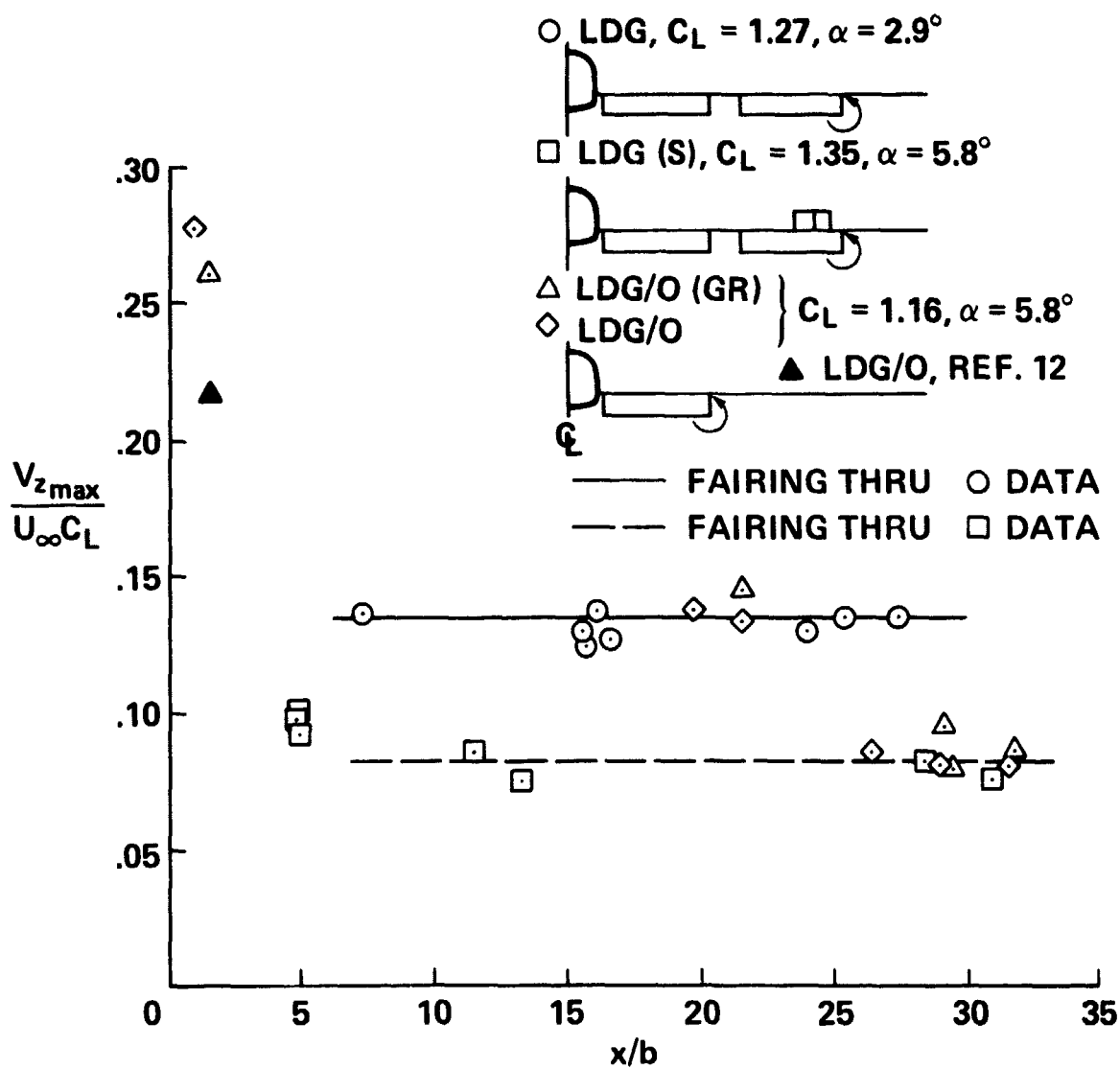


Figure 9.- Downstream dependence of flap vortex maximum tangential velocity.

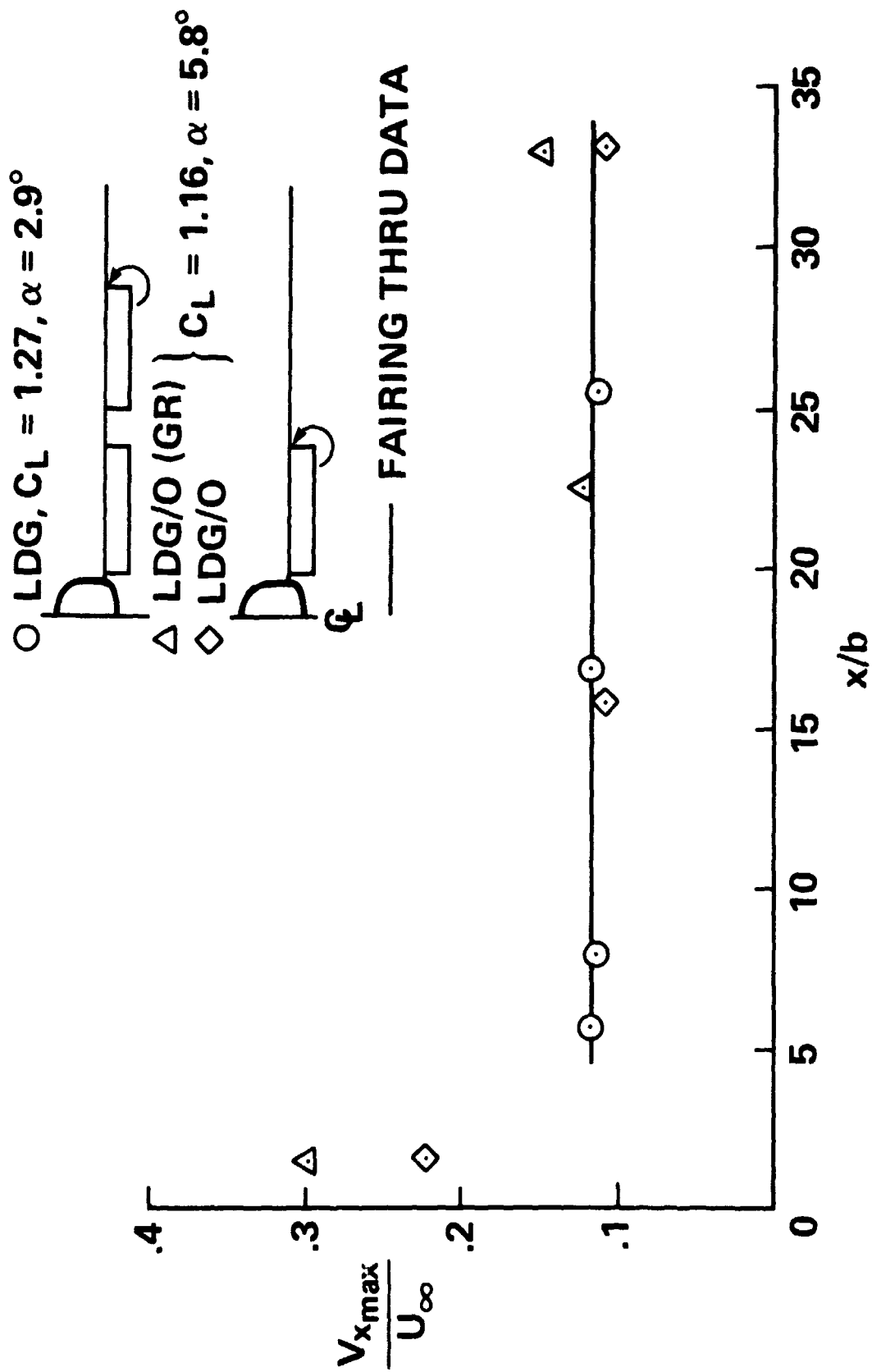


Figure 10.- Downstream dependence of flap vortex maximum axial velocity defect.

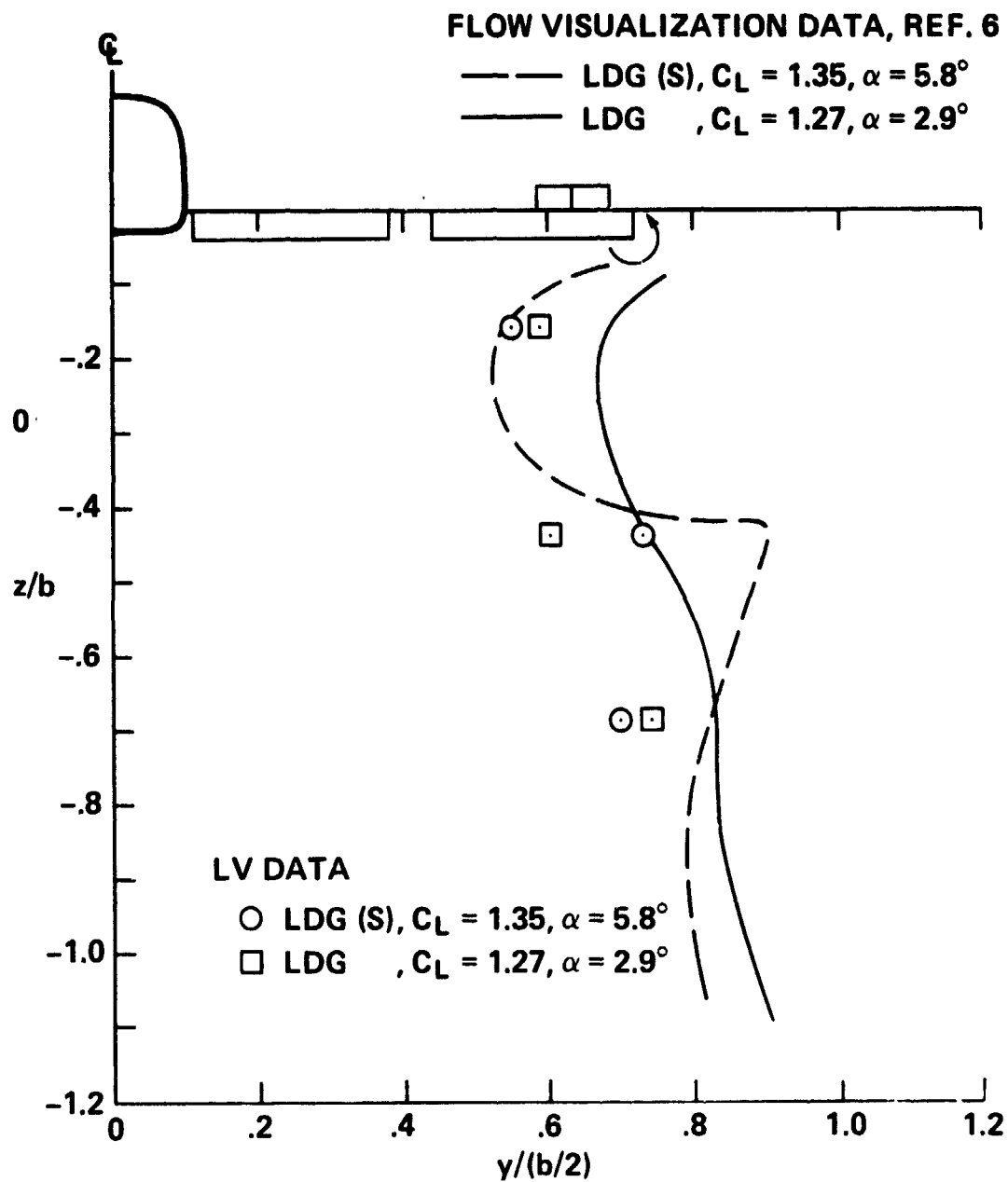


Figure 11.- Effect of flight spoilers on flap vortex trajectory. Landing configuration.

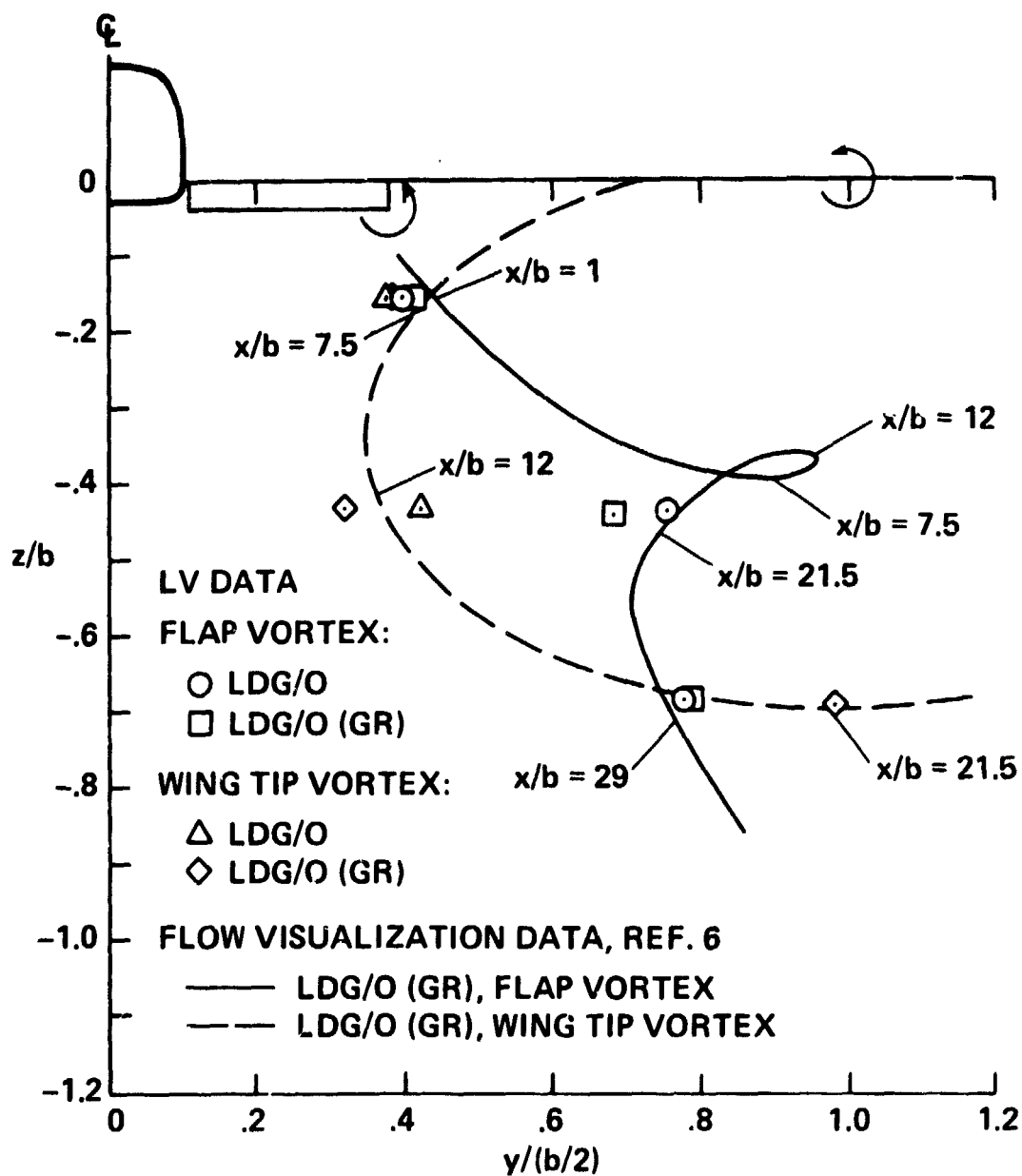


Figure 12.- Effect of landing gear on flap and wing tip vortex trajectories, $C_L = 1.16$, $\alpha = 5.8^\circ$.